Nitric Oxide Detection of Fe(DTC)$_3$-hybrizided CdSe Quantum Dots Via Fluorescence Energy Transfer

Chang-Yeoul Kim[*]

*Nano-composite Materials Center, Korea Institute of Ceramic Engineering and Technology,
101 Soho-ro Jinju-si Gyeongsangnam-do, Republic of Korea*

Abstract We successfully synthesize water-dispersible CTAB-capped CdSe@ZnS quantum dots with the crystal size of the CdSe quantum dots controlled from green to orange colors. The quenching effect of Fe(DTC)$_3$ is very efficient to turn off the emission light of quantum dots at four molar ratios of the CdSe quantum dots, that is, the effective covering the surface of quantum dots with Fe(DTC)$_3$. However, the reaction with Fe(DTC)$_3$ for more than 24 h is required to completely realize the quenching effect. The highly quenched quantum dots efficiently detect nitric oxide at nano-molar concentration of 110nM of NO with 34% of recovery of emission light intensity. We suggest that Fe(DTC)$_3$-hybridized CdSe@ZnS quantum dots are an excellent fluorescence resonance energy transfer probe for the detection of nitric oxide in biological systems.

Keywords: Quantum dot, CdSe, Nitric oxide, Detection, Fluorescence resonance energy transfer

1. Introduction

Nitric oxide (NO) is considered as an environmental toxic pollutant and also recognized as an important molecule that can regulate endothelial functions in the body. L-arginine was found to be the precursor for generation of NO which could be converted to L-citrulline by NO synthases (NOSs) in vivo. NO was involved in the variety of pathological and physiological functions such as endothelial vasorelaxation, cardiovascular functions, antimicrobial action, wound healing, tissue repair, neurotransmission, immune functions, blood pressure regulation, cytotoxicity, relaxation of the human penile corpus cavernosum, etc. [1-10] However, the mechanisms for these pathological and physiological roles of NO are not clear. So, to detect NO concentrations is important to understand the function of NO in biological systems with high selectivity and sensitivity. To investigate NO detection, a number of fluorescent probes have been developed in the last two decades [11-28]. The main categories are two, organic fluorescent probes and metal-ligand complex probes. Among the former, O-phenylenediamine(OPD)-based fluorescent probes have shown great potentials for the application in biological systems, and so some of them are commercially available. Because endogenous NO exists in low concentrations ($10^{-9} - 10^{-6}$ M) and short life time (seconds) in organisms, the rapid and highly selective reaction of fluorescent energy transfer detecting is required. In this work, we have developed CdSe quantum dots as a fluorophore for the NO detection. We synthesized ZnS@CdSe core/shell type quantum dots (QDs) and the QDs/complexes such as iron thiocarbamate (Fe(DTC)$_3$). In this paper, we suggest the highly effective CdSe quantum dot-based NO detection probe by the hybridization of Fe(DTC)$_3$ on CdSe quantum dots.

2. Experimental

2.1. Materials

The starting materials for the synthesis are CdO, selenium powder, stearic acid (SA), trioctylphosphine oxide (TOPO), tributylphosphine (TBP), hexadecylamine (HDA),

- 김창열: 책임연구원
*Corresponding Author: Chang-Yeoul Kim, **TEL:** +82-55-792-2707, **FAX:** +82-55-792-2730, **E-mail:** cykim15@kicet.re.kr

dodecylaminem and the solvents were hexane and methanol, which were purchased from Sigma-Aldrich.

2.2. The synthesis of CdSe quantum dots

Cd-SA complex was synthesized by reacting CdO with SA with each 0.2, and 0.8 mmol in three-neck flask in nitrogen flow. It was heated at 150°C to obtain a clear solution and then cooled to 80°C, after which 4.52 mmol of TOPO and 7.23 mmol of HAD were added and heated to 280°C for the fully dissolution of the chemicals. Then, Se solution (2 mmol) was injected into the Cd-SA precursor solution. The selenium solution was previously synthesized by a dissolution of selenium powder in TOP (2.36 mmol) and Hexadecene (5 ml) at 60°C in the glove box. To find out the crystal size of CdSe quantum dots, 2 ml of the product aliquots were taken every one minute at 280°C.

2.3. The synthesis of CdSe@ZnS quantum dot with core@shell structure

A core shell structured of CdSe@ZnS were synthesized for the stability of quantum dots. For the synthesis of ZnS solution, TOPO and HAD with 12.9 and 10.4 mmol, respectively, were put in the flask and the inner atmosphere was made as an inert by introducing nitrogen gas through Schlenk line. After CdSe quantum dots solution in hexane were added into the previous solution and then heated to 190°C. Then, ZnS shell solution were injected into CdSe quantum dots solution by syringe pump at 0.1 ml/min flow rate. The ZnS shell solution were synthesized by mixing zinc stearate (0.088~1.332 mmmol), sulfur powder (0.088~1.332 mmol), TOP (5 ml), toluene (2 ml) at 100°C. The reaction was conducted at 190°C for 1h and then washed using methanol and then dispersed in hexane.

2.4. Water-dispersible quantum dots by CTAB surface modification

CdSe@ZnS quantum dots were capped with hexadecyltrimethylammonium bromide (CTAB) as a cation surfactant for the dispersion in water. The structure of CTAB consists of hydrocarbon backbone and the heads of N^+ and Br^- ions. The hydrocarbon backbone is nonpolar with lipophilicity and the ions with hydrophilicity. To modify the surface of CdSe@ZnS, CdSe@ZnS quantum dots dispersed in hexane were evaporated to remove the solvent and then 0.55 mM CTAB solution added and reacted at 40°C for 20 min in the sonication bath.

2.5. NO detection of CdSe@ZnS quantum dots by Fluorescence Resonance Energy Transfer (FRET)

CTAB-capped CdSe@ZnS quantum dots were reacted with $Fe(II)(DTC)_3$ with 1:1, 1:2, and 1:4 molar ratio at 40°C for 24 h and then quenching effects of CdSe@ZnS quantum dots were observed. The fluorescence of CdSe quantum dots reacted with $Fe(II)(DTC)_3$ was characterized after the injection of the diethylamine NONOate sodium salt hydrate(DEA/NO). The fluorescence of the quantum dots for the detection of NO was analyzed with the fluorescence spectrometer (FluoroMate FS-2, Scinco., Korea).

3. Results

It is known that CdSe quantum dots have a different band gap energy with different crystal sizes. The visible light colors are violet (400-450 nm, 3.10-2.76) blue (450-490 nm, 2.76-2.53 eV), cyan (520-560 nm, 2.76-2.38 eV), green (520-560 nm, 2.38-2.21 eV), yellow (560-590 nm, 2.21-2.10 eV), orange (590-635 nm, 2.10-1.95 eV), and red (635-700 nm, 1.95-1.77 eV). CdSe quantum dots crystals reacted at 280°C for 1 to 10 min showed cyan, green to yellow. It is well known that CdSe quantum dot with 2, 4 and 8 nm sizes showed blue (480 nm), green (540 nm) and orange colors (600 nm) as shown in Fig. 1.
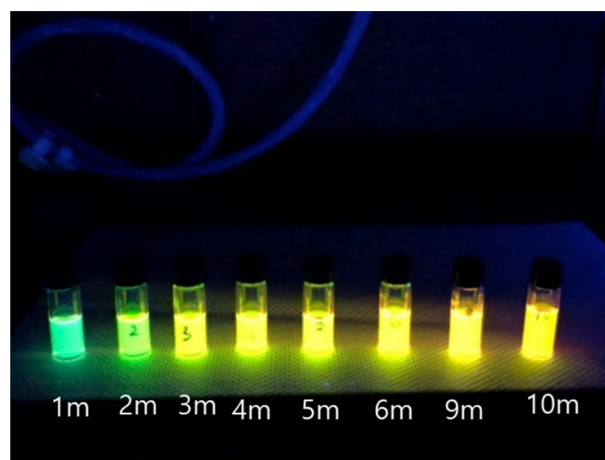

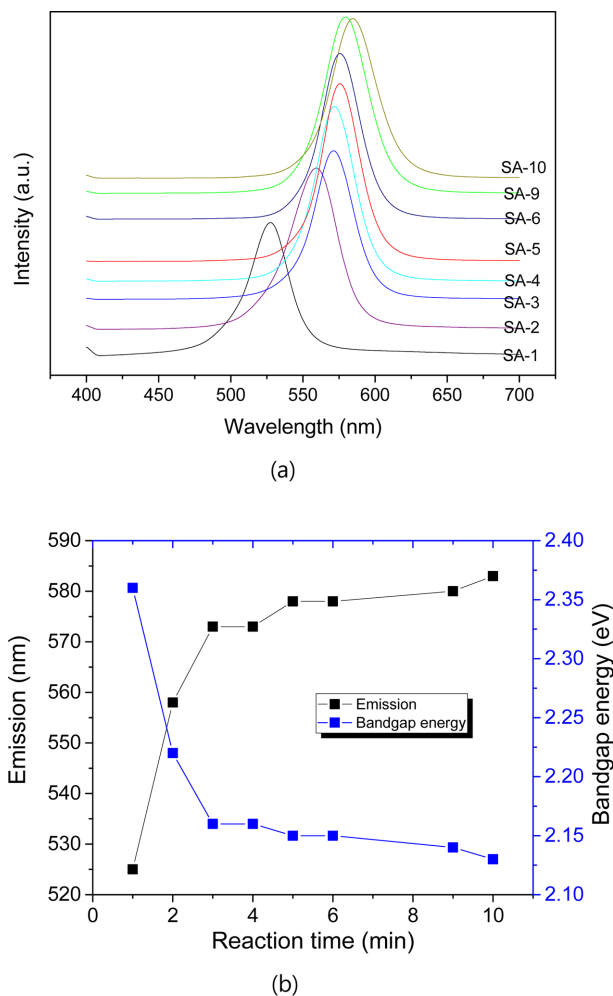**Fig. 1. QDs samples with various reaction times of 1, 2, 3, 4, 5, 6, 8, 10 min at 280°C.**

(a)

(b)

Fig. 2. PL speactra of QDs samples with various reaction times at 280°C.

Fig. 3. Change of PL spectra of the CdSe quantum dots after addition of Fe(DTC)$_3$.

Fluorescence spectra of the synthesized quantum dots are analyzed as shown in Fig. 2(a). The emission peaks of CdSe quantum dots are in the range of 525 and 595 nm. CdSe quantum dot crystals synthesized at 280°C for 1 min (SA-1, here the number means the reaction time) showed the emission peak at 525 nm (2.36 eV). CdSe quantum dots reacted for 2 min showed the emission peak at 558 nm (2.22 eV), 573 nm (2.16 eV) for 3 and 4 min, 578 nm (2.15 eV) for 5 and 6 min, 580 nm (2.14 eV) for 9 min and 583 nm (2.13 eV) for 10 min. As is shown in Fig. 2(b), we know that the variations of emission peak with reaction time increased from 525 for 1min to 573 nm for 3min and then saturated to 578 nm for more than 5 min. It is guessed that the crystal sizes of CdSe increased in the initial reaction state for 3 min and saturated after that. It is guessed that the crystal sizes of CdSe quantum dots are calculated by the equation, $D(nm)$
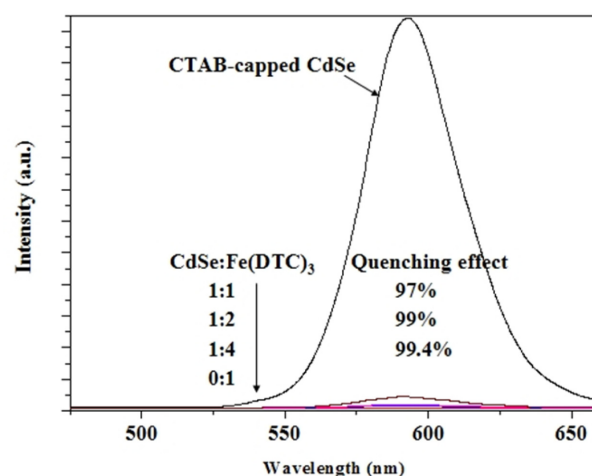
$= 59.60816 - 0.54736\lambda + 1.8873 \times 10^{-3}\lambda^2 - 2.85743 \times 10^{-6} \lambda^3 + 1.62974 \times 10^{-9} \lambda^4$ [29]. The crystal sizes are calculated as 2.76 nm for 525 nm, 3.36 nm for 558 nm, 3.74 nm for 573 nm, 3.88 nm for 578 nm, 3.94 nm for 580 nm and 4.03 nm for 583 nm.

Quenching effects of CTAB-capped CdSe with a reaction with metal complex of iron dithocarbamate (Fe(DTC)$_3$) were shown in Fig. 3. The binding of metal complex, Fe(DTC)$_3$, to CdSe quantum dots plays a role of excited electron transfer path, so that the ligand-bound CdSe quantum dots do not show any fluorescence emission peak by the irradiation of UV light, which is quenched (turn-off) state. We varied molar ratio of CdSe to Fe(DTC)$_3$ by 1:1, 1:2, and 1:4. Quenching effects could be evaluated by the decrease of emission peak. The quenching effects of Fe(DTC)$_3$ were 97% for 1:1, 99% for 1:2 and 99.4% for 1:4. So, the complexation of Fe(DTC)$_3$ to the surface of CTAB-capped CdSe quantum dots is almost covered to result in turning-off the emission light in the case of 1:2 and 1:3 molar ratio. Figure 4 shows the photoluminescence emission spectra of 11nM CdSe quantum dots reacted with 44 nM Fe(DTC)$_3$ in aqueous solution at 40°C with varied reaction time. It indicates that the quenching occurred in the initial reaction time of 1 h and it developed slowly in the reaction time from 1 to 24 h. After 24 h, the quenching effect was 99.4%, the maximum value, and it did not show any change after 24 h.
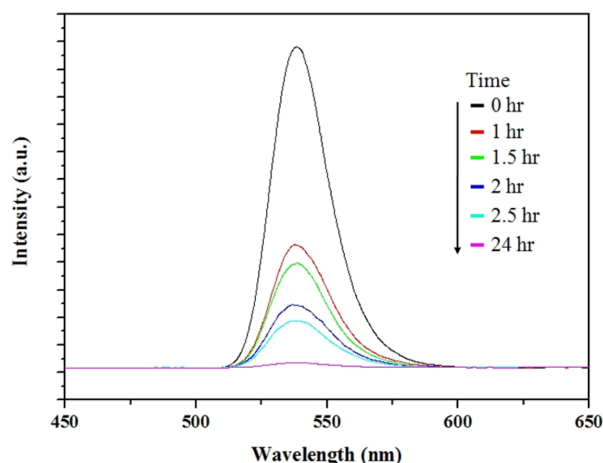
Figure 5 shows the photoluminescence emission spec-

Fig. 4. The intensity change of PL spectra of solutions mixed the CTAB-capped CdSe quantum dots and Fe(DTC)₃ as a function of the reaction time.
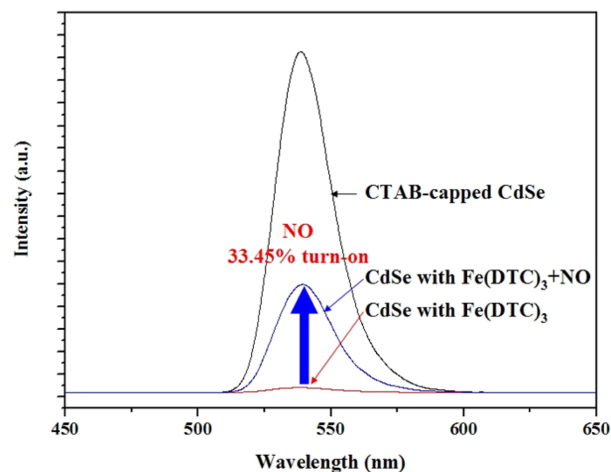

Fig. 5. The intensity change of PL spectra of the CdSe with Fe(DTC)₃ reacted with 110 nM DEA/NO.

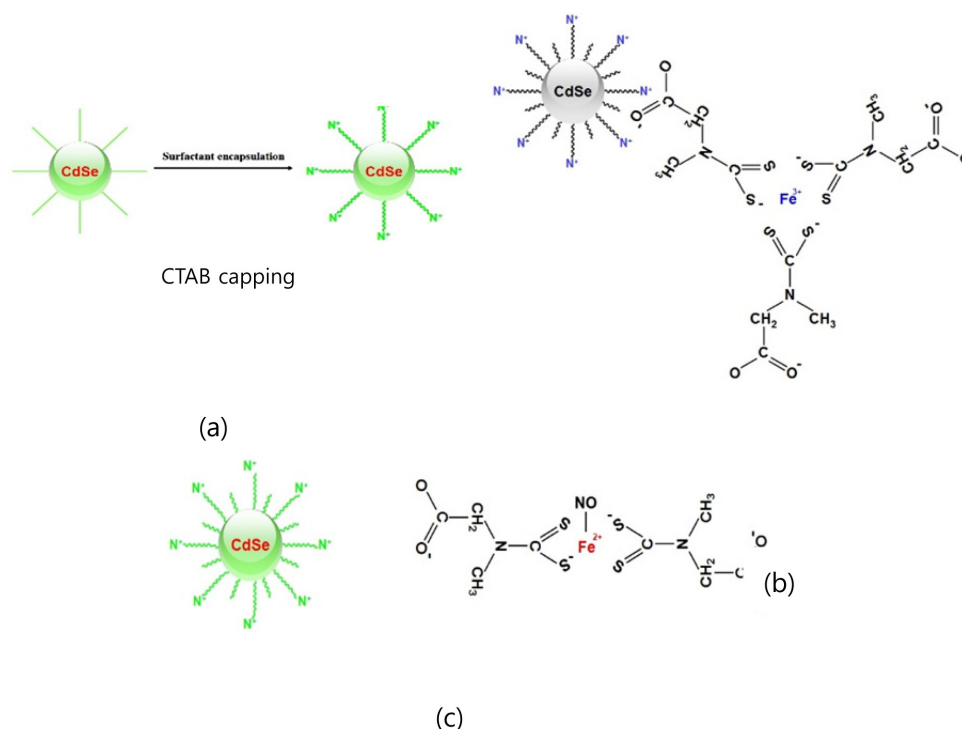**Fig. 6. Model structures of CTAB-capped CdSe@ZnS quantum dots fluorescence (a), Quenched state of Fe(DTC)3-hybridized CTAB-capped CdSe@ZnS quantum dots (b) and turn-on state of EDA/NO injection to the quenched quantum dots (c).**

tra of quenched CdSe quantum dots with Fe(DTC)₃ when 110 nM of DEA/NO was injected in argon atmosphere for the inhibition of oxidation of DEA/NO. The injection of DEA/NO showed 33.4% of turn on as shown in Fig. 5. It indicates that Fe(DTC)₃ hybridized CdSe quantum dots could play a role of biosensor to monitor NO quantities in biological system.

4. Discussion

Fluorescence resonance energy transfer (originally Förster resonance energy transfer; FRET) is energy transfer from donor to acceptor, CdSe quantum dot fluorophore and Fe(DTC)₃ in this paper. The FRET efficiency (E) depends on many physical parameters such as (1) the distance between the donor and the acceptor, (2) the

spectral overlap of the donor emission spectrum, and (3) the relative orientation of the donor emission dipole moment. In this study, the acceptor of Fe(DTC)$_3$ is not a fluorophore and so it plays only as an energy transfer path from the donor CdSe quantum dots. We suggested the model of fluorescent-state CTAB-capped CdSe quantum dots, quenched state of CdSe quantum dots hybridized with Fe(DTC)$_3$, and turn-on state of Fe(DTC)$_3$-complexed quenched CdSe quantum dots after the injection of DEA/NO. The rate of energy transfer (k_{ET}) can be expressed like the following equation. $k_{ET} = \left(\dfrac{R_0}{r}\right)^6 \dfrac{1}{\tau_D}$, where τ_D is the donor's fluorescence lifetime in the absence of the acceptor, R_0 being the Förster distance of this pair of donor and acceptor, i.e. the distance at which the energy transfer efficiency is 50% and r is the distance between donor and acceptor.

$$R_0^6 = \frac{9000\ln(10)Q_D k^2}{128\pi^5 n^4 N_A}\int_0^\infty \frac{F_D(\nu)\varepsilon_A(\nu)}{\nu^4}d\nu / \int_0^\infty F_D(\nu)d\nu$$

$$R_0^6 = 8.79\times10^{-25}n^{-4}Q_D k^2 J(\nu)cm^6$$

where Q_D is the fluorescence quantum yield of the donor in the absence of the acceptor, k^2 is the dipole orientation factor, n is the refractive index of the medium, N_A is the Avogadro constant, $\varepsilon_A(\nu)$ is the acceptor molar extinction coefficient, and $J(\nu)$ is the spectral overlap integral calculated as $\int_0^\infty \dfrac{F_D(\nu)\varepsilon_A(\nu)}{\nu^4}d\nu / \int_0^\infty F_D(\nu)\varepsilon_A d\nu$. Here, we use water as a medium with refractive index 1.33 and Q_D is 0.4 and $\varepsilon_A(\nu)$ is 1.14×10^4 mol^{-1}cm^{-1}, the wavelength of CdSe quantum dot emission is 540nm, then we obtained R_0 as 2.04 nm. So, the distance between the donor and the acceptor is longer than 2 nm to turn on the quenched CdSe quantum dots with Fe(DTC)$_3$. In the results of quenching effects of Fe(DTC)$_3$ with molar ratio, we obtained 4 molar ratio to CdSe. Based on this, we calculated the covering of Fe(DTC)$_3$ as 0.48 eaÅ^{-2}. In this study, Fe(DTC)$_3$ is a highly effective metal complex for the quenching of CdSe and the turn on by the injection DEA/NO. As is shown in Fig. 6. NO$^-$ is thought to bind Fe^{+2} ions so that the bond of CdSe as a donor and the acceptor of Fe(DTC)$_3$ is broken, indicating the distance between CdSe and Fe(DTC)$_3$ is longer than R_0.

5. Conclusions

We successfully synthesized water-dispersible CTAB-capped CdSe@ZnS quantum dots. We can control the crystal size of CdSe quantum dots with green to orange colors. The quenching effects of Fe(DTC)$_3$ is very efficient for four molar ratio to CdSe quantum dots, that is, the effective covering the surface of quantum dots. It is required that more than 24h of reaction of Fe(DTC)$_3$ for the full quenching effect. The highly quenched quantum dot shows the efficient detection of NO with nano-molar concentration.

Acknowledgments

References

[1] L. J. Ignarro, G. M. Buga, K. S. Wood, R. E. Byrns and G. Chaudhuri: Proc. Natl. Acad. Sci., USA, **84** (1987) 9265.

[2] R. M. J. Palmer, A. G. Ferrige and S. Moncada: Nature, **327** (1987) 524.

[3] J. Garthwaite: Eur. J. Neurosci., **27** (2008) 2783.

[4] C. Bogdan: Nat. Immunol., **2** (2001) 907.

[5] D. Fukumura, S. Kashiwagi and R. K. Jain: Nat. Rev. Cancer, **6** (2006) 521.

[6] S. Mocellin, V. Bronte and D. Nitti: Med. Res. Rev., **27** (2007) 317.

[7] H. Hong, J. Sun and W. Cai: Free Radical Biol. Med., **47** (2009) 684.

[8] G. Sivaraman, T. Anand and D. Chellappa: ChemPlusChem, **7** (2014) 1761.

[9] H. Yu, X. Zhang, Y. Xiao, W. Zou, L. Wang and L. Jin: Anal. Chem., **85** (2013) 7076.

[10] H. Yu, L. Jin, Y. Dai, H. Li and Y. Xiao: New J. Chem., **37** (2013) 1688.

[11] E. Koo and J.-C. Lee: J. of Nanomater., **27605** (2014) 1.

[12] L.-H. Yang, D. J. Ahn and E. Koo: Mater. Sci. Eng., C, **69** (2016) 625.

[13] L.-H. Yang, D. J. Ahn and E. Koo: BioChip, **12** (2018) 340.

[14] H. Yu, Y. Xiao and L. Jin: J. Am. Chem. Soc., **134** (2012) 17486.

[15] G. Sivaraman, T. Anand and D. Chellappa: Analyst, **137** (2012) 5881.

[16] G. Sivaraman, V. Sathiyaraja and D. Chellappa: J. Lumin., **145** (2014) 480.

[17] G. Sivaraman and D. Chellappa: J. Mater. Chem., B, **1** (2013) 5768.

[18] T. Nagano and T. Yoshimura: Chem. Rev., **102** (2002) 1235.

[19] M. H. Lim and S. J. Lippard: J. Am. Chem. Soc., **127** (2005) 12170.

[20] M. H. Lim, D. Xu and S. J. Lippard: Nat. Chem. Bio., **2** (2006) 375.

[21] S. Wang, M.-Y. Han and D. Huang: J. Am. Chem. Soc., **131** (2009) 11692.

[22] M. Han, X. Gao, J. Z. Su and S. Nie: Nat. Biotechnol., **19** (2001) 631.

[23] Y. Chan, J. P. Zimmer, M. Stroh, J. S. Steckel, R. K. Jain and M. G. Bawendi: Adv. Mater., **16** (2004) 2092.

[24] J. Yan, M. C. Estevez, J. E. Smith, K. Wang, X. He, L. Wang and W. Tana: Nano Today, **2** (2007) 44.

[25] X. Zhao, R. T.-Dytioco and W. Tan: J. Am. Chem. Soc., **125** (2003) 11474.

[26] D.-S. Lee, J.-C. Lee, E.-H. Koo and J.-H. Lee: J. Kor. Phys. Soc., **57** (2010) 1111.

[27] S. A. Hilderbrand and S. J. Lippard: Inorg. Chem., **43** (2004). 4674.

[28] M. H. Lim and S. J. Lippard: Inorg. Chem., **43** (2004) 6366.

[29] J. Jasieniak, L. Smith, J. Embden and P. Mulvaney and M. Califan: J. Phys. Chem., C, **113**(2009) 19468.